iScience

CellPress
OPEN ACCESS

Article

Tumor targeted 4-1BB agonist antibody-albumin fusions with high affinity to FcRn induce anti-tumor immunity without toxicity

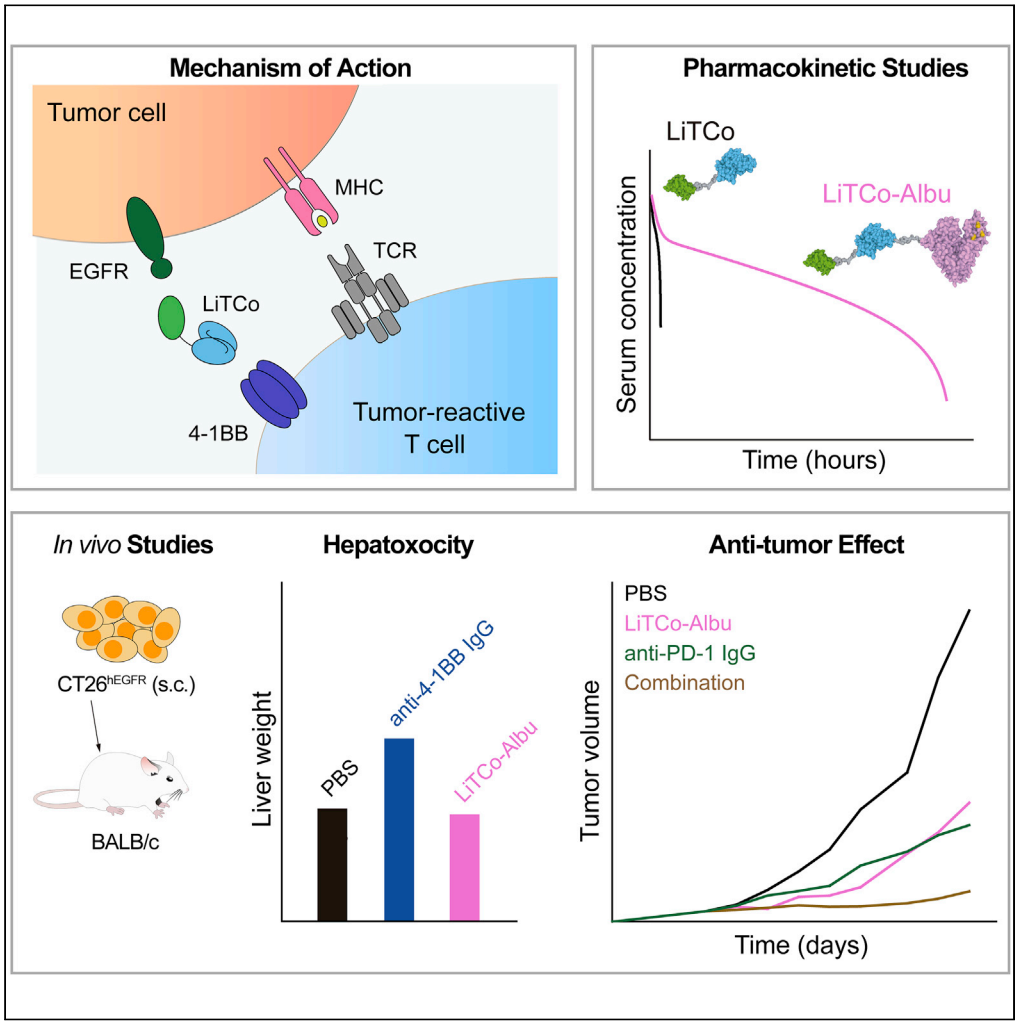

Oana Hangiu, Marta Compte, Anders Dinesen, ..., Laura Sanz, Kenneth A. Howard, Luis Álvarez-Vallina

lav.imas12@h12o.es

Highlights

Tumor targeted 4-1BB agonist antibody-albumin fusions with high affinity to FcRn

Potent EGFR-specific 4-1BB costimulation and FcRn-driven cellular recycling

Prolonged circulatory half-life and *in vivo* tumor inhibition, without toxicity

Combination with an anti-PD-1 blocking antibody further enhanced anti-tumor activity

Hangiu et al., iScience *25*, 104958
September 16, 2022
https://doi.org/10.1016/j.isci.2022.104958

iScience

CellPress
OPEN ACCESS

Article

Tumor targeted 4-1BB agonist antibody-albumin fusions with high affinity to FcRn induce anti-tumor immunity without toxicity

Oana Hangiu,[1,2,3] Marta Compte,[3] Anders Dinesen,[4] Rocio Navarro,[3] Antonio Tapia-Galisteo,[1,2] Ole A. Mandrup,[4] Ainhoa Erce-Llamazares,[1,2] Rodrigo Lázaro-Gorines,[1,2] Daniel Nehme-Álvarez,[1,2] Carmen Domínguez-Alonso,[1,2] Seandean L. Harwood,[5] Carlos Alfonso,[6] Belen Blanco,[1,2] Laura Rubio-Pérez,[1,2,7] Anaïs Jiménez-Reinoso,[1,2] Laura Díez-Alonso,[1,2] Francisco J. Blanco,[6] Laura Sanz,[8] Kenneth A. Howard,[4] and Luis Álvarez-Vallina[1,2,7,9,10,*]

SUMMARY

Costimulation of tumor-infiltrating T lymphocytes by anti-4-1BB monoclonal antibodies (mAbs) has shown anti-tumor activity in human trials, but can be associated with significant off-tumor toxicities involving FcγR interactions. Here, we introduce albumin-fused mouse and human bispecific antibodies with clinically favorable pharmacokinetics designed to confine 4-1BB costimulation to the tumor microenvironment. These Fc-free 4-1BB agonists consist of an EGFR-specific V_{HH} antibody, a 4-1BB-specific scFv, and a human albumin sequence engineered for high FcRn binding connected in tandem (LiTCo-Albu). We demonstrate *in vitro* cognate target engagement, EGFR-specific costimulatory activity, and FcRn-driven cellular recycling similar to non-fused FcRn high-binding albumin. The mouse LiTCo-Albu exhibited a prolonged circulatory half-life and *in vivo* tumor inhibition, with no indication of 4-1BB mAb-associated toxicity. Furthermore, we show a greater therapeutic effect when used in combination with PD-1-blocking mAbs. These findings demonstrate the feasibility of tumor-specific LiTCo-Albu antibodies for safe and effective costimulatory strategies in cancer immunotherapy.

INTRODUCTION

The development of cancer immunotherapy marks a milestone in the history of cancer therapy (Couzin-Frankel, 2013). One approach to enhance T cell-mediated anti-tumor immune responses relies on the monoclonal antibody (mAb)-blockade of inhibitory checkpoint receptors, such as cytotoxic T lymphocyte-associated protein 4 (CTLA-4) and the programmed cell death-1 (PD-1) receptor and its ligands, [programmed death-ligand 1 (PD-L1) and PD-L2 (Baumeister et al., 2016). A strategy that has resulted in outstanding efficacy in several cancer types, with tolerable toxicity profiles. The overall response rate, however, remains around 30% (Baumeister et al., 2016). Another approach involves the stimulation of costimulatory checkpoint receptors such as 4-1BB [also known as tumor necrosis factor receptor superfamily member 9 (TNFRSF9) or CD137)] (Melero et al., 2007). 4-1BB has only one known ligand [4-1BB-ligand (4-1BBL), TNFSF9], which is expressed on activated professional antigen-presenting cells (APCs), such as dendritic cells, macrophages, and activated B cells (Chester et al., 2018). When 4-1BB is bound by its natural ligand or an agonist mAb, it promotes the activation and proliferation of T cells, induction of cytolytic effector functions, and cell survival. Furthermore, 4-1BB costimulation on natural killer cells enhances cytokine release, and antibody-dependent cellular cytotoxicity (Kohrt et al., 2012; Wilcox et al., 2002). In preclinical studies, first-generation full-length 4-1BB agonistic mAbs have shown efficacy in several transplantable mouse tumors (Melero et al., 1997). However, off-tumor toxicities have been the major impediment to the clinical development of anti-4-1BB-agonistic IgGs, with several studies suggesting that toxicity is likely dependent on further crosslinking provided by Fc-Fc gamma receptor (FcγR) interactions (Compte et al., 2018; Li and Ravetch, 2013; Xu et al., 2003). The anti-human 4-1BB human IgG_4 urelumab (BMS-663513) showed clinical activity, but caused serious liver toxicity and was implicated in two patient deaths (Compte et al., 2018, 2021).

[1]Cancer Immunotherapy Unit (UNICA), Department of Immunology, Hospital Universitario12 de Octubre, 28041 Madrid, Spain

[2]Immuno-Oncology and Immunotherapy Group, Instituto de Investigación Sanitaria Hospital 12 de Octubre (imas12), 28041 Madrid, Spain

[3]Department of Antibody Engineering, Leadartis SL, Madrid, Spain

[4]Interdisciplinary Nanoscience Center (iNANO), Department of Molecular Biology and Genetics, Aarhus University, Aarhus C, Denmark

[5]Department of Molecular Biology and Genetics, Aarhus University, Aarhus C, Denmark

[6]Centro de Investigaciones Biológicas Margarita Salas (CIB), CSIC, Madrid 28040, Spain

[7]Chair for Immunology UFV/Merck, Universidad Francisco de Vitoria (UFV), 28223 Pozuelo de Alarcón, Madrid, Spain

[8]Molecular Immunology Unit, Hospital Universitario Puerta de Hierro Majadahonda, 28220 Majadahonda, Madrid, Spain

[9]Red Española de Terapias Avanzadas (TERAV), Instituto de Salud Carlos III (ISCII) (RICORS, RD21/0017/0030), Madrid, Spain

[10]Lead contact

*Correspondence: lav.imas12@h12o.es

https://doi.org/10.1016/j.isci.2022.104958

New strategies aiming to confine 4-1BB costimulation to the tumor microenvironment and avoid FcγR interactions are under clinical development (Claus et al., 2019; Compte et al., 2018, 2021; Hinner et al., 2019; Kamata-Sakurai et al., 2021; Mikkelsen et al., 2019). These approaches are based on bispecific molecules, targeting 4-1BB as well as tumor cells or tumor stromal cells (Claus et al., 2019; Compte et al., 2018, 2021; Hinner et al., 2019; Kamata-Sakurai et al., 2021), designed without Fc regions or with either engineered effector-silent Fc regions (Claus et al., 2019; Hinner et al., 2019) (Compte et al., 2018, 2021). Specific mutations introduced into the Fc region of antibodies can abrogate binding to FcɣRs with retained engagement with the neonatal Fc-receptor (FcRn) required for the long circulatory half-life of immunoglobulin G (IgG). An Fc silencing approach is complicated, however, by possible residual binding affinity by the "silenced" Fc regions owing to the existence of multiple FcɣRs (Vafa et al., 2014) and immunogenicity of the mutated Fc regions (Schlothauer et al., 2016). A fully synthetic constrained bicyclic peptide with bivalent 4-1BB binding and monovalent Nectin-4 binding, and a trispecific antibody constructed using single-chain variable fragments (scFv) against PD-L1, 4-1BB and human serum albumin (HSA) fusion are two Fc-free tumor target-dependent 4-1BB agonists shown to exhibit significant anti-tumor activity without liver toxicity. HSA has a circulatory half-life of ~19 days predominantly facilitated by a FcRn-driven endosomal cellular recycling pathway (Schmidt et al., 2017) but without the FcɣR and C1q binding associated with Fc fragments (Carson et al., 2014). The inclusion of the anti-HSA scFv in the trivalent design facilitates non-covalently association with the endogenous albumin pool, resulting in a plasma half-life of up to 2 weeks in non-human primates (Warmuth et al., 2021) compared to 2.3 h in mice for the bicyclic design (Hurov et al., 2021).

The inclusion of albumin-binding single-domain antibodies (sdAb) is a widely used half-life extension strategy (Hoefman et al., 2015), and Vobarilizumab (ALX-0061) a bispecific anti-IL-6 receptor (IL-6R) x anti-HAS tandem sdAb has reached phase IIb clinical trial (ClinicalTrials.gov). Non-covalent albumin binding, however, is susceptible to competition and displacement by endogenous ligands and other albumin binding drugs. Furthermore, drug-binding sites may overlap with the main FcRn binding interface in albumin domain III (Pilati and Howard, 2020). In contrast, the genetic fusion of drugs to recombinant HSA offers the opportunity to control and fine-tune the half-life of fusions by the inclusion of albumin sequences engineered with different FcRn binding affinities. Furthermore, drug fusion at HSA N-terminal located in domain I distant from the main binding interface preserves optimal FcRn engagement. Inspection of the binding interface of albumin with FcRn has allowed the design of recombinant variants with different FcRn affinities by single-point amino acid mutations (Andersen et al., 2012) that have been subsequently used to tune the pharmacokinetic (PK) profile (Andersen et al., 2014). Recently, we generated bispecific *light T cell engagers* (LiTEs) genetically fused to engineered HSA variants with different FcRn affinities to achieve programmable PK properties (Mandrup et al., 2021).

Here, we have generated a novel class of small-sized human and mouse tumor-specific 4-1BB-agonists coined *light T cell costimulatory* (LiTCo) antibodies composed of an anti-epidermal growth factor receptor (EGFR)-blocking single-domain V_{HH} and a 4-1BB-specific single-chain variable fragment (scFv) connected by a flexible peptide linker. Genetic fusion of a human albumin sequence engineered for high FcRn binding is used as a strategy to facilitate an extended plasma half-life (LiTCo-Albu). Both molecules showed potent costimulatory activity *in vitro* and showed tumor inhibition *in vivo*, with no indication of the 4-1BB mAb-associated toxicity. Furthermore, the combination of an EGFR-specific LiTCo-Albu with an immune checkpoint blocker (ICB) mAb resulted in a greater therapeutic effect.

RESULTS

Generation of tumor-targeted human light T cell costimulatory antibodies

In this study, we generated a small (≈47 kDa) human bispecific costimulatory antibody termed human LiTCo (hLiTCo, *light T cell costimulatory*) by fusing the anti-EGFR (human/mouse) EGa1 V_{HH} (Compte et al., 2020) to the N-terminal end of the anti-human 4-1BB SAP3.28 scFv (V_H-V_L orientation) (Compte et al., 2021) with a flexible GGGGS linker (Figures 1, S1A, and S1B). The hLiTCo-Albu was generated by genetic fusion of the hLiTCo to the N terminus of an albumin sequence with high binding to human FcRn ($Albumin^{HB}$) (Figures 1, S1C, and S1D) used previously by ourselves in an Albu-LiTE construct (Mandrup et al., 2021). Both hLiTCo and hLiTCo-Albu were efficiently secreted by human HEK293 cells, and in Western blot analysis under reducing conditions exhibited a migration pattern consistent with the molecular weights calculated from the amino acid sequences (Figure S2A). ELISA demonstrated that both antibodies specifically bound plastic-immobilized human EGFR (hEGFR) and human 4-1BB (h4-1BB) detected with anti-FLAG (hLiTCo and hLiTCo-Albu) or anti-HSA antibodies (hLiTCo-Albu) (Figures S2B and S2C). Both

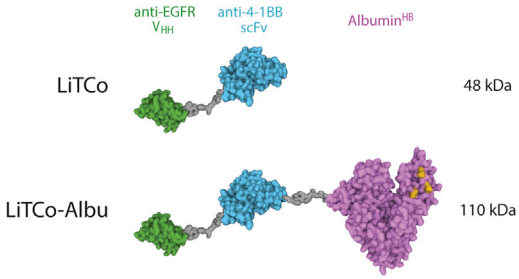

Figure 1. Schematic representation of EGFR-targeted human light T cell costimulatory (LiTCo) antibodies

The LiTCo molecule (48 kDa) comprises an anti-EGFR VHH (green) linked to an anti-4-1BB scFv (blue). In the LiTCo-Albu an engineered albumin variant (light purple) with enhanced binding ability to human FcRn (Albumin^{HB}) was genetically fused to the C-terminal end of the anti-4-1BB scFv and expressed as a single polypeptide (110 kDa).

antibodies were purified from the conditioned medium of transfected HEK293 cells by Strep-Tactin affinity chromatography yielding >90% pure protein when evaluated by Coomassie staining of reducing SDS-PAGE (Figure 2A). The purified hLiTCo and hLiTCo-Albu were obtained with yields of approximately 1 mg per liter of culture, and both antibodies were functionally active (Figures S3A and S3B) showing similar dose-dependent-binding curves against hEGFR and h4-1BB (Figures 2B and 2C). The binding was further confirmed by flow cytometry showing that both the EGFR- and 4-1BB-specific domains were active with no unspecific binding observed for the double-negative cell lines used (Figure S4).

Both hLiTCo and hLiTCo-Albu antibodies were evaluated for human FcRn binding at endosomal pH 5.5 using Bio-Layer Interferometry (BLI). The samples were compared to a non-fused FcRn-high binding recombinant Albumin^{HB} variant counterpart (Bern et al., 2020). The hLiTCo-Albu gave a good fit to a 1:1 binding model (Table S2), comparable to the non-fused Albumin^{HB}, while the hLiTCo resulted in no binding to FcRn at low pH; demonstrating that the observed binding signal is specific to the FcRn-albumin interaction (Figure 2D). An established cellular recycling assay (Schmidt et al., 2017) was used to compare human FcRn-driven cellular recycling of non-fused wild-type human albumin (Albumin^{WT}) and Albumin^{HB} variants with that of the hLiTCo-Albu. 5-fold more of the Albumin^{HB} was released back into the medium for the non-fused Albumin^{HB} compared with the Albumin^{WT} (Figure 2E). This effect was observed for the hLiTCo-Albu construct, with a higher concentration detected in the medium, possibly owing to anti-EGFR V_{HH} bound to hEGFR on the cell surface of the HMEC-1 cells (Mandrup et al., 2021) (Figure 2E).

The costimulatory activities of both antibodies were assessed using NFkB-luc2/4-1BB Jurkat reporter cells (Jurkat^{NFkB}) expressing cell surface h4-1BB and a luciferase reporter driven by a NFkB response element. Jurkat^{NFkB} cells were co-cultured with hEGFR-expressing target cells (3T3^{hEGFR}) or EGFR-negative wild-type 3T3 cells. In the presence of EGFR-mediated LiTCo cross-linking at the target cell surface, both constructs showed an approximately 20-fold increase of NFkB luciferase reporter activity at the highest concentration used (100 nM) (Figure 2F).

Generation of tumor-targeted mouse light T cell costimulatory antibodies

We replaced the anti-human 4-1BB SAP3.28 scFv with the anti-mouse 4-1BB 1D8 scFv (Compte et al., 2018) (Figures S1 and 1B) to investigate the anti-tumor effect and toxicity profile in immunocompetent mice. Both antibodies termed mouse LiTCo (mLiTCo) and mouse LiTCo-Albu (mLiTCo-Albu), were secreted by transfected HEK293 cells, and Western blot analysis demonstrated that under reducing conditions the migration patterns were single polypeptide chains with a molecular mass consistent with the calculated from their amino acid sequences (mLiTCo and mLiTCo-Albu, respectively) (Figure S5A). ELISA analysis demonstrated that both constructs specifically recognized hEGFR, mouse EGFR (mEGFR), and m4-1BB (Figures S5B and S5C). The conditioned medium from mLiTCo and mLiTCo-Albu stably transfected HEK293 cells was purified by Strep-Tactin affinity chromatography with protein yields of approximately 2 mg/L, which were >90% pure (Figure S6A). Analysis of the purified proteins by SEC shows major monomeric species for both of them, with no aggregates (Figure S6B). Using a set of globular proteins as molecular weight markers, the elution volumes of the antibodies yielded molar masses of 35 and 103 kDa for mLiTCo and mLiTCo-Albu, close to the estimated monomeric masses of 46.5 and 110.5 kDa (Figure S6B). The functionality and dose-dependence of the purified antibodies against immobilized hEGFR and m4-1BB were confirmed by ELISA (Figures S7A, S7B, 3A, and 3B), and the ability to detect both antigens when expressed on the cell surface was validated by flow cytometry (Figure S8). The FcRn-binding of mLiTCo and mLiTCo-Albu at pH 5.5 was investigated by BLI and compared to the corresponding albumin^{HB} variant (Bern et al., 2020). The BLI binding curves of mLiTCo-Albu fusion were qualitatively and quantitatively similar to the non-fused

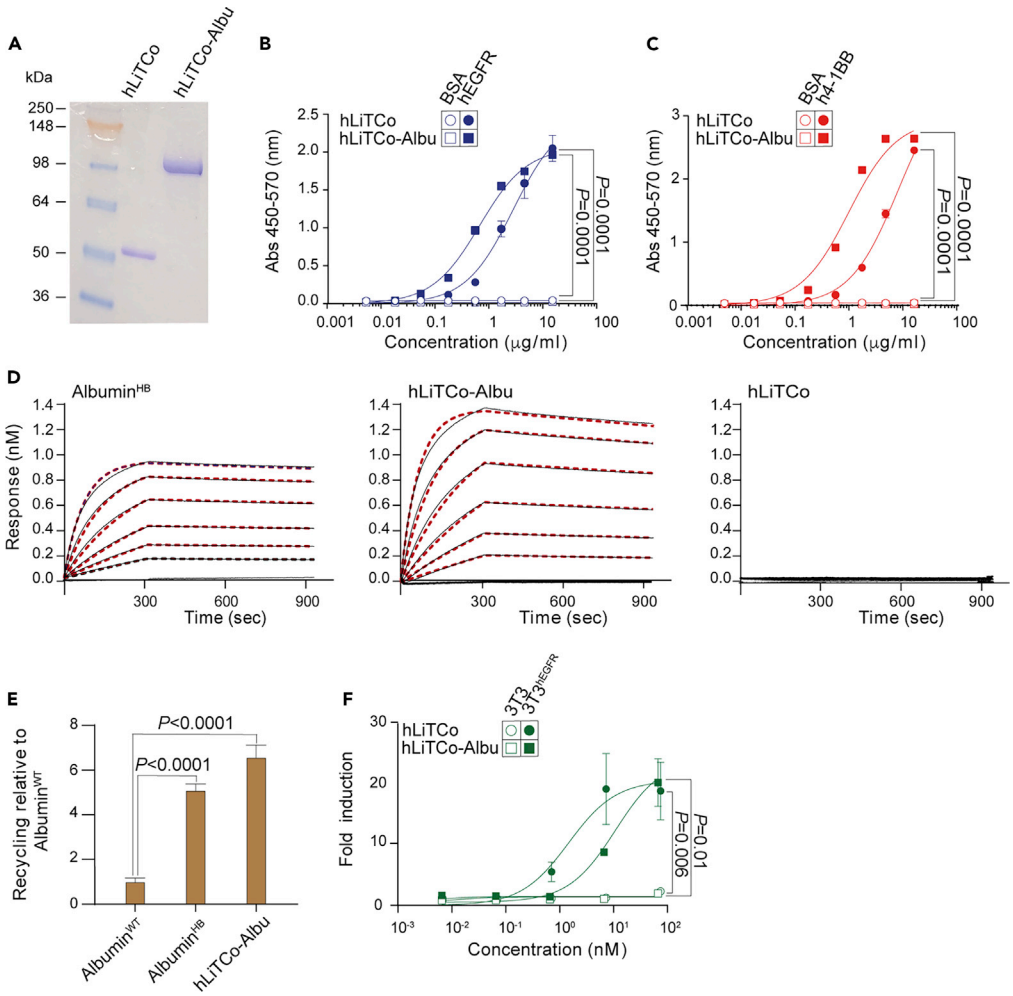

Figure 2. Functional characterization of hLiTCo and hLiTCo-Albu

Reducing SDS-PAGE of the purified hLiTCo and hLiTCo-Albu. Migration of molecular mass markers is indicated (kDa) (A). Saturation-binding curves with increasing concentrations of hLiTCo and hLiTCo-Albu against plastic immobilized hEGFR (B) or h4-1BB (C). Data are presented as mean ± SD (n = 3). Significance was calculated by an unpaired Student *t* test. BLI sensograms show association (0–300 s) and dissociation (300–900 s) of the respective analytes to immobilized human FcRn (D). The black line indicates baseline subtracted data while the dashed red line is the fit used to obtain the kinetic parameters based on a 1:1 binding model. ELISA detection of wild-type albumin (Albumin^{WT}), high-binding albumin (Albumin^{HB}), and hLiTCo-Albu following FcRn-mediated cellular recycling. The data are normalized to Albumin^{WT} and represented as mean ± SD. Significance was determined by unpaired Student *t* test. Jurkat^{NFkB} cells were co-cultured with NIH/3T3 or 3T3^{hEGFR} cells in the presence of increasing concentrations of hLiTCo or hLiTCo-Albu, and after 6 h at 37°C luminescence was determined (F). Data were presented as fold induction relative to the values obtained from unstimulated Jurkat^{NFkB} cells. Representative dose-concentration curves are presented and expressed as a mean ± SD (n = 3). Significance was determined by unpaired Student *t* test.

albumin^{HB} variant, while the mLiTCo did not exhibit any binding to human FcRn (Figure 3C). The mLiTCo-Albu was recycled in FcRn-expressing cells at levels similar to those observed with the non-fused albumin^{HB} variant (Figure 3D).

To study their costimulatory capacity primary mouse CD8a$^+$ T cells were stimulated with anti-mouse CD3 mAb and co-cultured with 3T3 or 3T3^{hEGFR} cells, in the presence of costimulatory antibodies (mLiTCo or mLiTCo-Albu) in solution. In the presence of 3T3 cells, the mLiTCo-Albu had a costimulatory effect similar to the IgG used as a control, but IFN-γ levels were greatly enhanced when 3T3^{hEGFR} cells were present (Figure 3E).

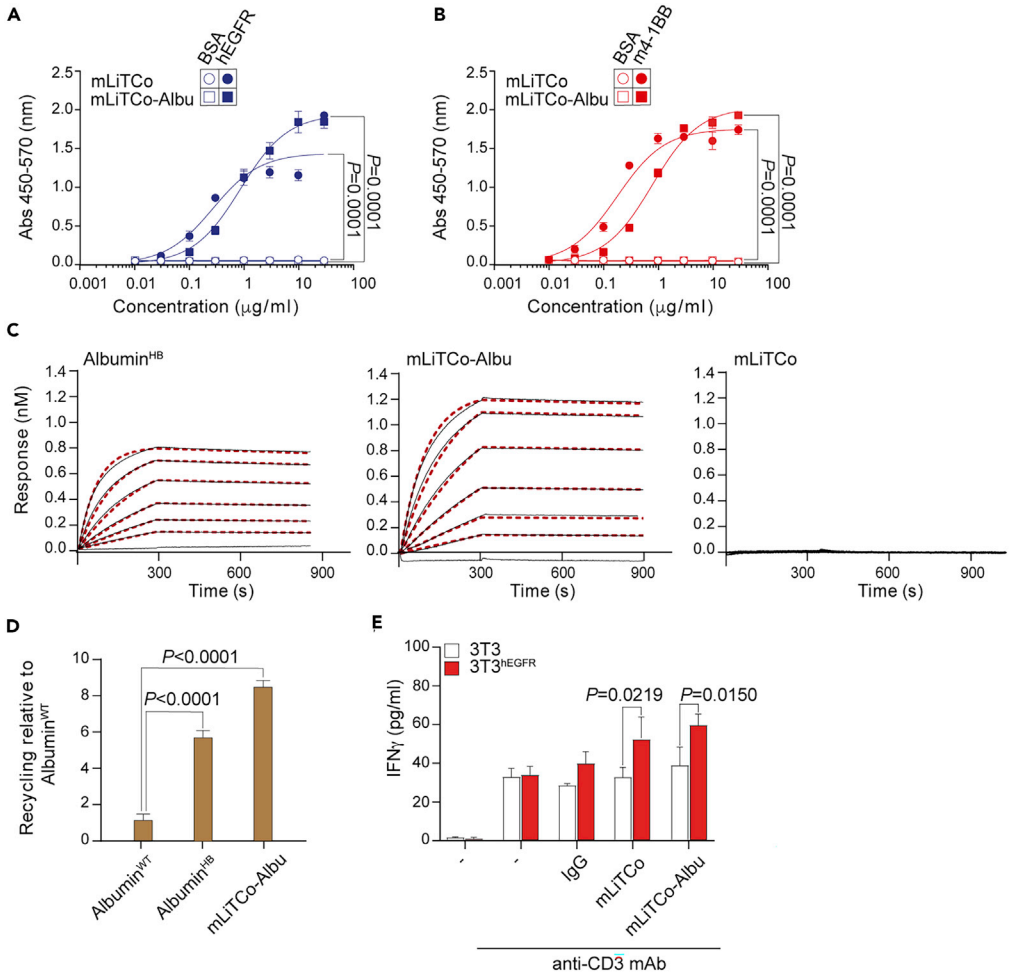

Figure 3. Characterization of purified mLiTCo and mLiTCo-Albu

Saturation-binding curves with increasing concentrations of mLiTCo and mLiTCo-Albu against plastic immobilized hEGFR (A) or m4-1BB (B). Data are presented as mean ± SD (n = 3). Significance was calculated by an unpaired Student *t* test. BLI sensorgrams show association (0–300 s) and dissociation (300–900 s) of the respective analytes to immobilized human FcRn (C). The black line indicates baseline subtracted data while the dashed red line is the fit used to obtain the kinetic parameters based on a 1:1 binding model. ELISA detection of wild-type albumin ($Albumin^{WT}$), high-binding albumin ($Albumin^{HB}$), and mLiTCo-Albu following FcRn-mediated cellular recycling (D). The data are normalized to $Albumin^{WT}$ and represented as mean ± SD. Significance was determined by unpaired Student *t* test. Mouse CD8a+ T cells were plated with anti-CD3 mAb and NIH/3T3 or $3T3^{hEGFR}$ cells in the presence of mLiTCo, mLiTCo-Albu, or IgG mAb. IFN-γ secretion was determined after 72 h (E). Data are expressed as mean ± SD (n = 3). Significance was calculated by an unpaired Student *t* test.

Pharmacokinetics of mouse light T cell costimulatory antibodies

mLiTCo and mLiTCo-Albu showed no significant loss of hEGFR and m4-1BB binding activity after 7 days in mouse serum at 37°C (Figure S9). Pharmacokinetic studies were performed in immunocompetent mice, which received a single intravenous (i.v.) injection of both constructs, and the amount of serum-active antibodies was quantified by ELISA. The mLiTCo was rapidly cleared from circulation with a terminal half-life of 0.17 h, whilst the mLiTCo-Albu showed a prolonged circulatory half-life of 30 h (Figure 4A and Table S3) that provided the basis for mLiTCo-Albu selection for anti-tumor efficacy studies.

Therapeutic activity and toxicity studies of mouse light T cell costimulatory-Albu

In order to determine the anti-tumor efficacy of mLiTCo-Albu antibody in immune-competent mice, we used gene-modified CT26 colorectal carcinoma cells expressing hEGFR ($CT26^{hEGFR}$). When tumors reached a diameter of 0.3 cm, anti-mouse 4-1BB IgG-based mAb 3H3 or mLiTCo-Albu were administered

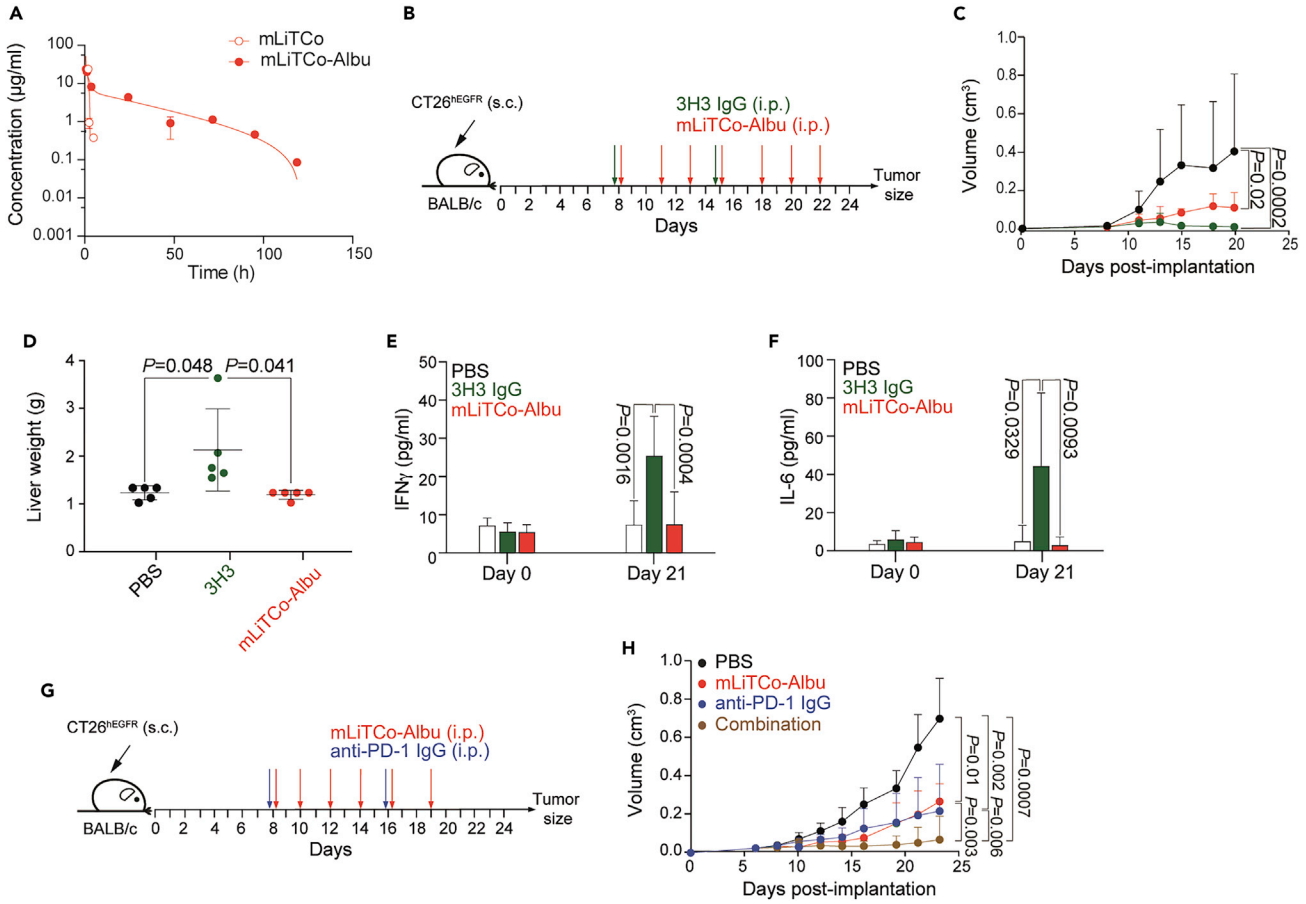

Figure 4. *In vivo* studies with mLiTCo-Albu

Pharmacokinetic study after a single intravenous (i.v.) dose (2 mg/kg) of mLiTCo (n = 3) and mLiTCo-Albu (n = 4) in BALB/c mice. Data are shown as mean ± SD (A). Average tumor volume growth of BALB/c mice bearing CT26^{hEGFR} tumors treated with PBS, anti-4-1BB 3H3 mAb, or mLiTCo-Albu. Data are presented as the mean ± SD Significance was determined by one-way ANOVA adjusted by the Bonferroni correction for multiple comparison test (B and C). Liver weights from mice (mean ± SD, n = 5/group) treated with PBS, anti-41BB 3H3 IgG mAb, or mLiTCo-Albu. Significance was determined by unpaired Student *t* test. (D). Sera from treated mice were collected from peripheral blood on days 0 and 21 of treatment, and levels of INF-γ (E) and IL-6 (F) were measured by ELISA (mean ± SD, n = 3 per time point). Significance was determined by unpaired Student *t* test. Average tumor volume growth of BALB/c mice bearing CT26^{hEGFR} tumors treated with PBS, mLiTCo-Albu, or anti-PD1 RMP 1.14 mAb alone or in combination (G and H). Data are presented as the mean ± SD. Significance was determined by one-way ANOVA adjusted by the Bonferroni correction for multiple comparison test.

(Figure 4B). Both treatments caused a significant delay in tumor growth (p = 0.0002 and p = 0.02, respectively) (Figures 4C and S10). We also studied the toxicity profile of the IgG-based 4-1BB agonist and mLiTCo-Albu. Treatment with anti-4-1BB IgG resulted in a significant increase in liver weight (p = 0.04) (Figure 4D), and elevation of INFγ and IL-6 in serum (p = 0.001 and p = 0.03, respectively; Figures 4E and 4F) than PBS-treated mice. In contrast, treatment with mLiTCo-Albu did not result in hepatomegaly (p = 0.04; Figure 4D), and the levels of inflammatory cytokines were comparable to those found in PBS-treated animals (Figures 4E and 4F). The therapeutic effect of combining mLiTCo-Albu with an anti-PD-1 blocker mAb was investigated in the same mouse model (Figure 4G). Both mLiTCo-Albu and anti-PD-1 IgG monotherapy were able to reduce tumor development (p = 0.01 and p = 0.002, respectively; Figure 4H). Moreover, the combination therapy of anti-PD1 mAb plus mLiTCo-Albu was superior to both monotherapies and resulted in an additional decrease in tumor growth (p = 0.0007; Figure 4H), and regression in 4 out of 6 (66%) mice bearing CT26^{hEGFR} tumors (Figure S11).

DISCUSSION

This work introduces a new generation of small-sized tumor-specific 4-1BB-agonists (LiTCo) that can be engineered for an extended circulatory half-life by genetic fusion to a human albumin sequence with

high affinity for human FcRn (LiTCo-Albu). Both molecules efficiently bind 4-1BB and EGFR, with the functionality of the anti-4-1BB binding domain not compromised by the C-terminal addition of the albumin^{HB} sequence in the LiTCo-Albu design. Both hLiTCo and hLiTCo-Albu are strictly dependent on the presence of EGFR to induce 4-1BB signaling in an h4-1BB-reporting cell line. Moreover, when the study was conducted under near physiologic conditions using primary mouse CD8$^+$ T cells, the mLiTCo and mLiTCo-Albu did not provide effective 4-1BB costimulation without additional EGFR-mediated cross-linking. Previous studies have suggested a function for 4-1BB costimulation in organizing TCR/CD3-mediated signaling at the immune synapse (Nam et al., 2005), and the size and architecture of this type of molecule may be well-suited to the context of immunological synapsis (Roda-Navarro and Álvarez-Vallina, 2019).

To date, the generation of Fc-free molecules (Compte et al., 2018, 2021) or molecules bearing effector-silent Fc domains (Claus et al., 2019; Hinner et al., 2019) have been the standard strategies employed in all ongoing clinical trials. However, it is possible that mutations introduced to engineer silenced Fc regions may compromise antibody stability and immunogenicity (Schlothauer et al., 2016), and do not completely avoid residual FcγR binding activities (Vafa et al., 2014). The removal or mutations of the Fc may result in compromised FcRn engagement and concomitant short circulatory half-life and more frequent dosing. The inclusion of albumin-binding domains is a promising strategy to utilize the endogenous albumin pool (Pilati and Howard, 2020), but it does not allow the engineering of improved traits into albumin. Moreover, the binding of these domains might be reduced by other endogenous and exogenous albumin ligands, and without careful design, the binding site may overlap with albumin's main FcRn binding interface in domain III (Pilati and Howard, 2020). The generation of engineered human albumin variants with different FcRn affinities (Andersen et al., 2012), offers a tool-set to modulate the PK properties of the designer antibodies (Andersen et al., 2014). Moreover, fusion at albumin N-terminus, in albumin domain I distant from the main binding interface, preserves the binding characteristics of these sequences. This strategy has recently been successfully applied to EGFR-specific T cell engagers and validated in a physiologically relevant hFcRn+/+, hAlb+/+ model (Mandrup et al., 2021). The two LiTCo-Albu constructs generated in this study showed similar FcRn binding and FcRn-driven *in vitro* cellular recycling characteristics to non-fused albumin^{HB}. The mLiTCo-Albu exhibited an extended circulatory half-life of 30 h in mice compared to 0.17 h of the mLiTCo. It expected that this could be further extended using in a model with the appropriate hFcRn+/+, hAlb+/+ phenotype (Viuff et al., 2016).

LiTCo-Albu possess both active and passive tumor-targeting properties through its interaction with EGFR (Compte et al., 2018), and albumin receptor-mediated processes in a caveolae-dependent manner (Desai et al., 2006). Furthermore, FcRn overexpression in tumors and increased accumulation in tumor-bearing mice of an albumin variant with high affinity to FcRn have recently been documented (Larsen et al., 2020), supporting possible FcRn-mediated tumor-targeting. The ability of albumin to disseminate through the lymphatic system has been exploited for T cell activation in tumor-associated locoregional lymph nodes (Liu et al., 2014; Ma et al., 2019). Colorectal cancer infiltrated lymph nodes showed higher scores of EGFR staining than control groups (Mokhtari et al., 2012). This suggests that EGFR-targeted LiTCo-Albu could have the potential in treating primary and disseminated cancers. Here, we show that LiTCo-Albu monotherapy provided significant anti-tumor activity in immunocompetent mice bearing established CT26^{hEGFR} tumors. Furthermore, the combination of the EGFR-specific mLiTCo-Albu with an anti-PD-1 blocking antibody further enhanced anti-tumor activity, resulting in complete regression in more than 60% of mice. Importantly, treatment with mLiTCo-Albu did not induce systemic inflammatory cytokine production or hepatotoxicity typically associated with IgG-based anti-4-1BB agonists. These results further strengthen the association between immunological abnormalities/organ toxicities and Fc-FcγR interactions.

In summary, we have engineered Fc-free tumor-specific LiTCo albumin fusions with extended circulatory half-life provided by the high FcRn affinity of the included albumin sequence. These LiTCo albumin fusions exhibit improved anti-tumor effects in immunocompetent mice, without the systemic and liver toxicity associated with first-generation anti-4-1BB agonistic IgG mAbs. These findings are highly relevant for the development of next-generation immunotherapeutic agents targeting 4-1BB and emphasize the need for additional studies with tumor-specific human LiTCo-Albu in order to confirm the therapeutic potential of this novel 4-1BB costimulation strategy.

Limitations of the study

The main limitation is the absence of suitable humanized animal models that would allow the detailed study of the therapeutic efficacy and toxicity of the tumor-specific costimulatory molecules generated in this work.

STAR★METHODS

Detailed methods are provided in the online version of this paper and include the following:

- KEY RESOURCES TABLE
- RESOURCE AVAILABILITY
  - Lead contact
  - Materials availability
  - Data and code availability
- EXPERIMENTAL MODEL AND SUBJECT DETAILS
  - Mice
  - Cells and culture conditions
- METHOD DETAILS
  - Construction of expression vectors
  - Expression, purification and characterization of recombinant antibodies
  - Western blotting
  - ELISA
  - Flow cytometry
  - FcRn binding kinetics assessment by Bio-Layer Interferometry
  - FcRn-mediated cellular recycling assay
  - 4-1BB-dependent NF-kB activation assay
  - Antigen specific T cell costimulation assay
  - Serum stability
  - Pharmacokinetics study
  - Therapeutic studies
- QUANTIFICATION AND STATISTICAL ANALYSIS
  - Statistical analysis

SUPPLEMENTAL INFORMATION

Supplemental information can be found online at https://doi.org/10.1016/j.isci.2022.104958.

ACKNOWLEDGMENTS

Financial support for this work was obtained from the MCIN/AEI/10.13039/501100011033 (SAF2017-89437-P and PDC2021-121711-100 to LA-V, PID2019-104544GB-I00 to CA, and PID2020-113225GB-I00 to FJB), partially supported by the European Regional Development Fund (ERDF); the Carlos III Health Institute (ISCIII) (PI19/00132 to LS; PI20/01030 to BB), partially supported by the ERDF; the ISCIII-RICORS within the Next Generation EU program (plan de Recuperación, Transformación y Resilencia); the Spanish Association Against Cancer (AECC 19084 to LA-V); the CRIS Cancer Foundation (FCRIS-2018-0042 and FCRIS-2021-0090 to LA-V), the BBVA Foundation (Ayudas Fundación BBVA a Equipos de Investigación Científica SARS-CoV-2 years COVID-19 to LA-V); and the Fundació "La Caixa" (HR21-00761 project IL7R_LungCan to LA-V). AD, OAM, and KAH were funded by the Novo Nordisk Foundation, Grant; CEMBID (Center for Multifunctional Biomolecular Drug Design, Grant Number: NNF17OC0028070). OH was supported by an industrial PhD fellowship from the Comunidad de Madrid (IND2020/BMD-17668). AE-L was supported industrial PhD fellowship from the Carlos III Health Institute (IFI18/00045). CD-A was supported by a predoctoral fellowship from the Spanish Ministry of Science Innovation and Universities (PRE2018-083445). LR-P was supported by a predoctoral fellowship from the Immunology Chair, Universidad Francisco de Vitoria/Merck. LD-A was supported by a Rio Hortega fellowship from the Carlos III Health Institute (CM20/00004).

AUTHOR CONTRIBUTIONS

Conceptualization, K.A.H. and L.A-V.; Methodology, O.H., M.C., A.D.; R.N.; A.T-G.; O.A.M., A.E-L; D.N-A.; C.D-A.; S.L.H.; L.R-P.; A.J-R.; and L.D-A.; Investigation, O.H., M.C., A.D.; R.N.; A.T-G.; O.A.M., A.E-L; D.N-A.; C.D-A.; S.L.H.; C.A.; B.B., L.R-P.; A.J-R.; L.D-A.; F.J.B; and L.S. Writing – Original Draft, O.H. and

L.A-V.; Writing – Review & Editing, O.H.; M.C.; A.D.; O.A.M.; S.L.H.; B.B.; A.J-R.; F.J.B.; L.S.; K.A.H. and L.A-V.; Funding Acquisition, B.B.; L.S.; C.A.; F.J.B; K.A.H. and L.A-V.

DECLARATION OF INTERESTS

L.S. and L.A-V. are co-founders of Leadartis. M.C. and R.N. are current employees of Leadartis. The remaining authors declare no competing interests.

Received: February 4, 2022
Revised: July 21, 2022
Accepted: August 12, 2022
Published: September 16, 2022

REFERENCES

Andersen, J.T., Dalhus, B., Cameron, J., Daba, M.B., Plumridge, A., Evans, L., Brennan, S.O., Gunnarsen, K.S., Bjørås, M., Sleep, D., and Sandlie, I. (2012). Structure-based mutagenesis reveals the albumin-binding site of the neonatal Fc receptor. Nat. Commun. *3*, 610. https://doi.org/10.1038/ncomms1607.

Andersen, J.T., Dalhus, B., Viuff, D., Ravn, B.T., Gunnarsen, K.S., Plumridge, A., Bunting, K., Antunes, F., Williamson, R., Athwal, S., et al. (2014). Extending serum half-life of albumin by engineering neonatal Fc receptor (FcRn) binding. J. Biol. Chem. *289*, 13492–13502. https://doi.org/10.1074/jbc.M114.549832.

Baumeister, S.H., Freeman, G.J., Dranoff, G., and Sharpe, A.H. (2016). Coinhibitory pathways in immunotherapy for cancer. Annu. Rev. Immunol. *34*, 539–573. https://doi.org/10.1146/annurev-immunol-032414-112049.

Bern, M., Nilsen, J., Ferrarese, M., Sand, K.M.K., Gjølberg, T.T., Lode, H.E., Davidson, R.J., Camire, R.M., Bækkevold, E.S., Foss, S., et al. (2020). An engineered human albumin enhances half-life and transmucosal delivery when fused to protein-based biologics. Sci. Transl. Med. *12*, eabb0580. https://doi.org/10.1126/scitranslmed.abb0580.

Carson, J.M., Okamura, K., Wakashin, H., McFann, K., Dobrinskikh, E., Kopp, J.B., and Blaine, J. (2014). Podocytes degrade endocytosed albumin primarily in lysosomes. PLoS One *9*, e99771. https://doi.org/10.1371/journal.pone.0099771.

Chester, C., Sanmamed, M.F., Wang, J., and Melero, I. (2018). Immunotherapy targeting 4-1BB: mechanistic rationale, clinical results, and future strategies. Blood *131*, 49–57. https://doi.org/10.1182/blood-2017-06-741041.

Claus, C., Ferrara, C., Xu, W., Sam, J., Lang, S., Uhlenbrock, F., Albrecht, R., Herter, S., Schlenker, R., Hüsser, T., et al. (2019). Tumor-targeted 4-1BB agonists for combination with T cell bispecific antibodies as off-the-shelf therapy. Sci. Transl. Med. *11*, eaav5989. https://doi.org/10.1126/scitranslmed.aav5989.

Compte, M., Harwood, S.L., Erce-Llamazares, A., Tapia-Galisteo, A., Romero, E., Ferrer, I., Garrido-Martin, E.M., Enguita, A.B., Ochoa, M.C., Blanco, B., et al. (2021). An Fc-free EGFR-specific 4-1BB-agonistic trimerbody displays broad antitumor activity in humanized murine cancer models without toxicity. Clin. Cancer Res. *27*, 3167–3177. https://doi.org/10.1158/1078-0432.CCR-20-4625.

Compte, M., Harwood, S.L., Martínez-Torrecuadrada, J., Perez-Chacon, G., González-García, P., Tapia-Galisteo, A., Van Bergen En Henegouwen, P.M.P., Sánchez, A., Fabregat, I., Sanz, L., et al. (2020). Case report: an EGFR-targeted 4-1BB-agonistic trimerbody does not induce hepatotoxicity in transgenic mice with liver expression of human EGFR. Front. Immunol. *11*, 614363. https://doi.org/10.3389/fimmu.2020.614363.

Compte, M., Harwood, S.L., Muñoz, I.G., Navarro, R., Zonca, M., Perez-Chacon, G., Erce-Llamazares, A., Merino, N., Tapia-Galisteo, A., Cuesta, A.M., et al. (2018). A tumor-targeted trimeric 4-1BB-agonistic antibody induces potent anti-tumor immunity without systemic toxicity. Nat. Commun. *9*, 4809. https://doi.org/10.1038/s41467-018-07195-w.

Couzin-Frankel, J. (2013). Breakthrough of the year 2013. Cancer immunotherapy. Science *342*, 1432–1433. https://doi.org/10.1126/science.342.6165.1432.

Desai, N., Trieu, V., Yao, Z., Louie, L., Ci, S., Yang, A., Tao, C., De, T., Beals, B., Dykes, D., et al. (2006). Increased antitumor activity, intratumor paclitaxel concentrations, and endothelial cell transport of cremophor-free, albumin-bound paclitaxel, ABI-007, compared with cremophor-based paclitaxel. Clin. Cancer Res. *12*, 1317–1324. https://doi.org/10.1158/1078-0432.CCR-05-1634.

Hinner, M.J., Aiba, R.S.B., Jaquin, T.J., Berger, S., Dürr, M.C., Schlosser, C., Allersdorfer, A., Wiedenmann, A., Matschiner, G., Schüler, J., et al. (2019). Tumor-Localized costimulatory T-cell engagement by the 4-1BB/HER2 bispecific antibody-anticalin fusion PRS-343. Clin. Cancer Res. *25*, 5878–5889. https://doi.org/10.1158/1078-0432.CCR-18-3654.

Hoefman, S., Ottevaere, I., Baumeister, J., and Sargentini-Maier, M. (2015). Pre-clinical intravenous serum pharmacokinetics of albumin binding and non-half-life extended nanobodies®. Antibodies *4*, 141–156. https://doi.org/10.3390/antib4030141.

Hurov, K., Lahdenranta, J., Upadhyaya, P., Haines, E., Cohen, H., Repash, E., Kanakia, D., Ma, J., Kristensson, J., You, F., et al. (2021). BT7480, a novel fully synthetic Bicycle tumor-targeted immune cell agonist™ (Bicycle TICA™) induces tumor localized CD137 agonism. J. Immunother. Cancer *9*, e002883. https://doi.org/10.1136/jitc-2021-002883.

Kamata-Sakurai, M., Narita, Y., Hori, Y., Nemoto, T., Uchikawa, R., Honda, M., Hironiwa, N., Taniguchi, K., Shida-Kawazoe, M., Metsugi, S., et al. (2021). Antibody to CD137 activated by extracellular adenosine triphosphate is tumor selective and broadly effective in vivo without systemic immune activation. Cancer Discov. *11*, 158–175. https://doi.org/10.1158/2159-8290.CD-20-0328.

Kohrt, H.E., Houot, R., Weiskopf, K., Goldstein, M.J., Scheeren, F., Czerwinski, D., Colevas, A.D., Weng, W.-K., Clarke, M.F., Carlson, R.W., et al. (2012). Stimulation of natural killer cells with a CD137-specific antibody enhances trastuzumab efficacy in xenotransplant models of breast cancer. J. Clin. Invest. *122*, 1066–1075. https://doi.org/10.1172/JCI61226.

Larsen, M.T., Mandrup, O.A., Schelde, K.K., Luo, Y., Sørensen, K.D., Dagnæs-Hansen, F., Cameron, J., Stougaard, M., Steiniche, T., and Howard, K.A. (2020). FcRn overexpression in human cancer drives albumin recycling and cell growth; a mechanistic basis for exploitation in targeted albumin-drug designs. J. Control. Release *322*, 53–63. https://doi.org/10.1016/j.jconrel.2020.03.004.

Li, F., and Ravetch, J.V. (2013). Antitumor activities of agonistic anti-TNFR antibodies require differential FcγRIIB coengagement in vivo. Proc. Natl. Acad. Sci. USA *110*, 19501–19506. https://doi.org/10.1073/pnas.1319502110.

Liu, H., Moynihan, K.D., Zheng, Y., Szeto, G.L., Li, A.V., Huang, B., Van Egeren, D.S., Park, C., and Irvine, D.J. (2014). Structure-based programming of lymph-node targeting in molecular vaccines. Nature *507*, 519–522. https://doi.org/10.1038/nature12978.

Ma, L., Dichwalkar, T., Chang, J.Y.H., Cossette, B., Garafola, D., Zhang, A.Q., Fichter, M., Wang, C., Liang, S., Silva, M., et al. (2019). Enhanced CAR-T cell activity against solid tumors by vaccine boosting through the chimeric receptor. Science *365*, 162–168. https://doi.org/10.1126/science.aav8692.

Mandrup, O.A., Ong, S.C., Lykkemark, S., Dinesen, A., Rudnik-Jansen, I., Dagnæs-Hansen, N.F., Andersen, J.T., Alvarez-Vallina, L., and Howard, K.A. (2021). Programmable half-life and anti-tumour effects of bispecific T-cell engager-albumin fusions with tuned FcRn affinity.

Commun. Biol. *4*, 310. https://doi.org/10.1038/s42003-021-01790-2.

Melero, I., Hervas-Stubbs, S., Glennie, M., Pardoll, D.M., and Chen, L. (2007). Immunostimulatory monoclonal antibodies for cancer therapy. Nat. Rev. Cancer *7*, 95–106. https://doi.org/10.1038/nrc2051.

Melero, I., Shuford, W.W., Newby, S.A., Aruffo, A., Ledbetter, J.A., Hellström, K.E., Mittler, R.S., and Chen, L. (1997). Monoclonal antibodies against the 4-1BB T-cell activation molecule eradicate established tumors. Nat. Med. *3*, 682–685. https://doi.org/10.1038/nm0697-682.

Mikkelsen, K., Harwood, S.L., Compte, M., Merino, N., Mølgaard, K., Lykkemark, S., Alvarez-Mendez, A., Blanco, F.J., and Álvarez-Vallina, L. (2019). Carcinoembryonic antigen (CEA)-Specific 4-1BB-costimulation induced by CEA-targeted 4-1BB-agonistic trimerbodies. Front. Immunol. *10*, 1791. https://doi.org/10.3389/fimmu.2019.01791.

Mokhtari, M., Ardestani, M.M., and Movahedipour, M. (2012). An immunohistochemical study of EGFR expression in colorectal cancer and its correlation with lymph nodes status and tumor grade. J. Res. Med. Sci. *17*, 741–744.

Nam, K.-O., Kang, H., Shin, S.-M., Cho, K.-H., Kwon, B., Kwon, B.S., Kim, S.-J., and Lee, H.-W. (2005). Cross-linking of 4-1BB activates TCR-signaling pathways in CD8+ T lymphocytes. J. Immunol. *174*, 1898–1905. https://doi.org/10.4049/jimmunol.174.4.1898.

Pilati, D., and Howard, K.A. (2020). Albumin-based drug designs for pharmacokinetic modulation. Expert Opin. Drug Metab. Toxicol. *16*, 783–795. https://doi.org/10.1080/17425255.2020.1801633.

Pozzi, C., Cuomo, A., Spadoni, I., Magni, E., Silvola, A., Conte, A., Sigismund, S., Ravenda, P.S., Bonaldi, T., Zampino, M.G., et al. (2016). The EGFR-specific antibody cetuximab combined with chemotherapy triggers immunogenic cell death. Nat. Med. *22*, 624–631. https://doi.org/10.1038/nm.4078.

Roda-Navarro, P., and Álvarez-Vallina, L. (2019). Understanding the spatial topology of artificial immunological synapses assembled in T cell-redirecting strategies: a major issue in cancer immunotherapy. Front. Cell Dev. Biol. *7*, 370. https://doi.org/10.3389/fcell.2019.00370.

Schlothauer, T., Herter, S., Koller, C.F., Grau-Richards, S., Steinhart, V., Spick, C., Kubbies, M., Klein, C., Umaña, P., and Mössner, E. (2016). Novel human IgG1 and IgG4 Fc-engineered antibodies with completely abolished immune effector functions. Protein Eng. Des. Sel. *29*, 457–466. https://doi.org/10.1093/protein/gzw040.

Schmidt, E.G.W., Hvam, M.L., Antunes, F., Cameron, J., Viuff, D., Andersen, B., Kristensen, N.N., and Howard, K.A. (2017). Direct demonstration of a neonatal Fc receptor (FcRn)-driven endosomal sorting pathway for cellular recycling of albumin. J. Biol. Chem. *292*, 13312–13322. https://doi.org/10.1074/jbc.M117.794248.

Vafa, O., Gilliland, G.L., Brezski, R.J., Strake, B., Wilkinson, T., Lacy, E.R., Scallon, B., Teplyakov, A., Malia, T.J., and Strohl, W.R. (2014). An engineered Fc variant of an IgG eliminates all immune effector functions via structural perturbations. Methods *65*, 114–126. https://doi.org/10.1016/j.ymeth.2013.06.035.

Viuff, D., Antunes, F., Evans, L., Cameron, J., Dyrnesli, H., Thue Ravn, B., Stougaard, M., Thiam, K., Andersen, B., Kjærulff, S., and Howard, K.A. (2016). Generation of a double transgenic humanized neonatal Fc receptor (FcRn)/albumin mouse to study the pharmacokinetics of albumin-linked drugs. J. Control. Release *223*, 22–30. https://doi.org/10.1016/j.jconrel.2015.12.019.

Warmuth, S., Gunde, T., Snell, D., Brock, M., Weinert, C., Simonin, A., Hess, C., Tietz, J., Johansson, M., Spiga, F.M., et al. (2021). Engineering of a trispecific tumor-targeted immunotherapy incorporating 4-1BB co-stimulation and PD-L1 blockade. OncoImmunology *10*, 2004661. https://doi.org/10.1080/2162402X.2021.2004661.

Wilcox, R.A., Tamada, K., Strome, S.E., and Chen, L. (2002). Signaling through NK cell-associated CD137 promotes both helper function for $CD8^+$ cytolytic T cells and responsiveness to IL-2 but not cytolytic activity. J. Immunol. *169*, 4230–4236. https://doi.org/10.4049/jimmunol.169.8.4230.

Xu, Y., Szalai, A.J., Zhou, T., Zinn, K.R., Chaudhuri, T.R., Li, X., Koopman, W.J., and Kimberly, R.P. (2003). Fc gamma Rs modulate cytotoxicity of anti-Fas antibodies: implications for agonistic antibody-based therapeutics. J. Immunol. *171*, 562–568. https://doi.org/10.4049/jimmunol.171.2.562.

STAR★METHODS

KEY RESOURCES TABLE

REAGENT or RESOURCE	SOURCE	IDENTIFIER
Antibodies		
Mouse monoclonal anti-FLAG (clone M2)	Sigma-Aldrich	Cat#F3165 RRID:AB_259529
HRP-conjugated anti-FLAG mAb (clone M2)	Abcam	Cat# ab49763 RRID:AB_869428
Goat polyclonal anti-mouse IgG Horseradish peroxidase (HRP)-conjugated	Sigma-Aldrich	Cat#A2554 RRID:AB_258008
Goat polyclonal anti-mouse IgG Horseradish peroxidase (HRP)-conjugated	Jackson ImmunoResearch	Cat#115-035-166 RRID:AB_2338511
Sheep polyclonal anti-human serum albumin Horseradish peroxidase (HRP)-conjugated	Abcam	Cat#ab8941 RRID:AB_306876
Goat polyclonal anti-mouse R-Phycoerythrin AffiniPure F(ab')$_2$ Fragment, Fcγ fragment specific	Jackson ImmunoReserach	Cat#115-116-071 RRID:AB_2338626
Goat anti-Albumin	Sigma-Aldrich	Cat#A7544 RRID:AB_258350
Armenian Hamster monoclonal anti-mouse CD3ε (clone 145-2C11)	Immuno-step	Cat#MO3PU RRID:N/A
Mouse monoclonal anti-FLAG Horseradish peroxidase (HRP)-conjugated (clone M2)	Abcam	Cat#ab49763 RRID:AB_869428
Anti-mouse 4-1BB (CD137) IgG (clone 3H3)	BioXCell	Cat#BE0239 RRID:AB_2687721
Anti-mouse PD-1 (CD279) IgG (clone RMP 1.14)	BioXCell	Cat#BE0146 RRID:AB_10949053
Chemicals, peptides, and recombinant proteins		
Recombinant human EGFR	Peprotech	Cat#AF-100-15
Recombinant human EGFR Fc Chimera	R&D	Cat#344-ER
Recombinant mouse EGFR His Tag	SinoBiological	Cat#51091-M08H
Recombinant human 4-1BB/TNFRSF9 Fc chimera	R&D	Cat#838-4B
Recombinant mouse 4-1BB/CD137 Fc chimera	SinoBiological	Cat#50811-M02H
Biotinylated human FcRn	Immunitrack	Cat#ITF01
Mouse IgG1$_\kappa$	Biolegend	Cat#401402
FcRn wild-type-binding albumin	Sigma-Aldrich	Cat#A6608
Streptavidin	Sartorius	Cat#18-5019
Critical commercial assays		
Mouse CD8a$^+$ T cell Isolation Kit	Miltenyi Biotec	Cat#130-095-236
Murine IFN-γ ELISA Set	Diaclone	Cat#861.050.005
Mouse IL-6 Matched Antibody Pair ELISA Kit	Abcam	Cat#ab213749
Mycoplasma Gel Detection Kit	Biotools	Cat#90.021-4542
Promega Bio-Glo™ Luciferase Assay System	Promega	Cat#G7941
Experimental models: Cell lines		
Human: HEK293 cells	ATCC	CRL-1573 RRID:CVCL_0045
Human: HEK293T cells	ATCC	CRL-11268 RRID:CVCL_1926
Human: HEK293 cells expressing mouse 4-1BB	Provided by Prof I. Melero (CIMA, Pamplona, Spain)	N/A
Mouse: NIH/3T3 cells	ATCC	CRL-1658 RRID:CVCL_0594

(*Continued on next page*)

Continued

REAGENT or RESOURCE	SOURCE	IDENTIFIER
Mouse: NIH/3T3 expressing human EGFR cells	Provided by Dr A. Villalobo (IIBm, Madrid, Spain)	N/A
Mouse: CT26 cells	ATCC	CRL-2638 RRID:CVCL_7256
Mouse: CT26 expressing human EGFR cells	Pozzi et al., 2016	N/A
HMEC-1 expressing FcRn cells	Schmidt et al., 2017	N/A
GloResponse™NFkB-*luc2*/4-1BB Jurkat	Promega	Cat#JA2351
Experimental models: Organisms/strains		
Female BALB/cOlaHsd	Envigo	Cat#162
Oligonucleotides		
FwCMV (CGCAAATGGGCGGTAGGCGTG)	Thermo Scientific	Cat#12744-017
RvBGH (TAGAAGGCACAGTCGAGG)	Thermo Scientific	Cat#N57502
Recombinant DNA		
pCR3.1-FLAG-strepII-EGa1-SAP3.28	This paper	N/A
pCR3.1-FLAG-strepII-EGa1-SAP3.28-Albumin^{HB}	This paper	N/A
pCR3.1-FLAG-strepII-EGa1-1D8	This paper	N/A
pCR3.1-FLAG-strepII-EGa1-1D8-Albumin^{HB}	This paper	N/A
Software and algorithms		
Studio Lite software	Li-Cor	https://www.licor.com/bio/image-studio-lite
Prism 8.4.0	GraphPad	https://www.graphpad.com
Prism 9.0.0	GraphPad	https://www.graphpad.com
FlowJo X	FlowJo	https://www.flowjo.com/solutions/flowjo
Octet System Data Analysis 10.0.1.6	Sartorius	https://www.sartorius.com/en/products/protein-analysis/octet-bli-detection/octet-systems-software?utm_source=google&utm_medium=cpc&utm_campaign=Octet&utm_term=dynamic_ads&utm_content=search&gclid=Cj0KCQjwg_iTBhDrARIsAD3Ib5hnE2-XKJsSC5xWTgg6ZDuPcNbNz6vtTe1Um6IX4gAcegCc-51llGkaAuRfEALw_wcB

RESOURCE AVAILABILITY

Lead contact

Further information and reasonable requests for resources and reagents should be directed to the lead contact, Luis Álvarez-Vallina (lav.imas12@h12o.es).

Materials availability

All reagents used in this study will be made available upon reasonable request to the lead contact, Luis Álvarez-Vallina (lav.imas12@h12o.es).

Data and code availability

- All data reported in this paper will be shared by the lead contact (lav.imas12@h12o.es) upon request.
- This paper does not report original code.
- Any additional information required to reanalyze the data reported in this paper is available from the lead contact (lav.imas12@h12o.es) upon request.

EXPERIMENTAL MODEL AND SUBJECT DETAILS

Mice

Six-weeks female BALB/cOlaHsd (referred as BALB/c) were purchased from Envigo. Animals were housed in controlled conditions of temperature (21 ± 1°C), humidity (50 ± 5%), and 12 h light/dark cycles. Animals were maintained under specific-pathogen-free condition and sterilized water and food were available *ad libitum*. All animal procedures conformed to European Union Directive 86/609/EEC and Recommendation 2007/526/EC, enforced in Spanish law under RD 1201/2005. Animal protocols were performed in strict adherence to the guidelines stated in the International Guiding Principles for Biomedical Research Involving Animals, established by the Council for International Organizations of Medical Sciences (CIOMS) and were approved by the Ethics Committee of Animal Experimentation of the Instituto Investigación Sanitaria Puerta de Hierro-Segovia de Arana (Hospital Universitario Puerta de Hierro Majadahonda, Madrid, Spain). Procedures were additionally approved by the Animal Welfare Division of the Environmental Affairs Council of the Government of Madrid (076/19).

Cells and culture conditions

HEK293 (CRL-1573), HEK293T (CRL-11268) and NIH/3T3 (CRL-1658) were obtained from American Type Culture Collection (ATCC) (Rockville, MD, USA). NIH/3T3 cells expressing human EGFR (3T3hEGFR) were kindly provided by Dr A. Villalobo (IIBm, Madrid, Spain). Mouse CT26 cells (CRL-2638) infected with *p*-BABEpuro-hEGFR expressing human EGFR ($CT26^{hEGFR}$) were provided by Dr M. Rescigno (European Institute of Oncology, Milan) (Pozzi et al., 2016). Cells were grown in Dulbecco's modified Eagle's medium (DMEM, Gibco) supplemented with 2 mM L-glutamine (Lonza), 10% (v/v) heat inactivated fetal bovine serum (FBS, Gibco), and antibiotics (100 units/mL penicillin, 100 mg/mL streptomycin) (Pen/Strep, Gibco), referred as to DMEM complete medium (DCM), at 37°C in 5% CO2 humidity. HEK293 cells expressing mouse 4-1BB ($HEK293^{m4-1BB}$) were obtained from Prof I. Melero (CIMA, Pamplona, Spain) and the h4-1BB expressing HEK293 cell line ($HEK239^{h4-1BB}$) was previously generated (Compte et al., 2021) and selected in DCM with 500 μg/mL Geneticin (G418, Gibco). HMEC-1-FcRn (FcRn-transduced human microvascular endothelial cell line-1) cells were previously generated (Schmidt et al., 2017) and grown in MCDB 131 medium (Gibco) with 10 ng/mL human EGFR (Preprotech), 1 μg/mL hydrocortisone (Merck), 50 μg/mL Geneticin (G418), 0.25 μg/mL Puromycin (Gibco), 2 mM L-glutamine, and with 10% FBS. The cell lines were routinely screened for mycoplasma contamination by PCR using the Mycoplasma Gel Detection Kit.

METHOD DETAILS

Construction of expression vectors

To generate the human LiTCo (hLiTCo) (FLAG-strepII-EGa1-SAP3.28) construct, the SAP3.28 scFv gene sequence (Compte et al., 2021) was inserted into the pCR3.1-EGa1 expression vector using NotI/XbaI restriction enzymes. FLAG-strepII-EGa1-SAP3.28 DNA sequence was subcloned as AgeI/SnaBI into the vector containing the high affinity FcRn binding human albumin ($Albumin^{HB}$) (Bern et al., 2020), resulting in the FLAG-strepII-EGa1-SAP3.28-AlbuminHB construct, hereafter referred to as hLiTCo-Albu. A synthetic gene encoding DNA fragment FLAG-strepII-EGa1 was synthesized by Geneart AG and ligated as HindIII/NotI into pCR3.1-1D8 expression vector to generate the mouse LiTCo (mLiTCo) (FLAG-strepII-EGa1-1D8) construct. The mLiTCo-Albu (FLAG-strepII-EGa1-1D8-AlbuminHB) construct was obtained after subcloning the FLAG-strepII-EGa1-1D8 sequence as AgeI/SnaBI into the aforementioned HB expression vector (Bern et al., 2020). All the sequences were verified using primers FwCMV and RvBGH (Table S1).

Expression, purification and characterization of recombinant antibodies

HEK293 cells were transfected with the appropriate expression vectors using Lipofectamine 3000 reagent (Invitrogen) and selected in DCM containing 500 μg/mL Geneticin (G418) to generate stable cell lines HEK293-hLiTCo, HEK293-hLiTCo-Albu, HEK293-mLiTCo and HEK293-mLiTCo-Albu. Conditioned media were collected and purified using Strep-Tactin purification system (IBA Lifesciences) using an ÄKTA Go system (Cytiva). The purified antibodies were dialyzed overnight at 4°C against PBS Phosphate-Buffered Saline (PBS, Corning) with 150 mM NaCl at pH 7.0, analyzed by 12% SDS-PAGE under reducing conditions and stored at 4°C. Size exclusion chromatography was performed on a Superdex 200 Increase 10/300 GL column (Cytiva) on and AKTA-GO chromatography system (Cytiva). 50 μL of the solutions at 0.15 (mLiTCo) or 0.07 g/L (mLiTCo-Albu) were injected into the column and run at room temperature in PBS pH 7.4, with a flow rate of 0.5 mL/min.

Western blotting

Protein samples were separated under reducing conditions on 10–20% Tris-glycine gels (Invitrogen) and transferred to nitrocellulose membranes and probed with anti-FLAG (clone M2; F3165, Sigma-Aldrich) mAb (1 μg/mL), washed and incubated with horseradish peroxidase (HRP)-conjugated goat anti-mouse IgG (GAM-HRP) (1:10,000 dilution) (Sigma-Aldrich). Visualization of protein bands was performed with the ChemiDoc Gel Imaging System (Bio Rad). Images were analyzed with Image Studio Lite software.

ELISA

Maxisorp immunoplates (NUNC Brand Products) were coated with human EGFR-human IgG1 Fc chimera (hEGFR) (R&D) or mouse EGFR His Tag (mEGFR) (SinoBiological), and human 4-1BB IgG1 Fc chimera (h4-1BB) (R&D) or mouse 4-1BB-human IgG1 Fc chimera (m4-1BB) (SinoBiological) (3 μg/mL) overnight at 4°C. After washing and blocking with 5% bovine serum albumin (BSA, Sigma-Aldrich) or 5% nonfat dry milk (NFDM) in PBS, 100 μL of conditioned media from transfected HEK293 cells or purified antibody solution (1 μg/mL) was added and incubated for 1 h at room temperature. After washing, anti-FLAG mAb (1 μg/mL) (clone M2; F3165, Sigma-Aldrich) was added for 1 h incubation at room temperature. The plates were washed and 100 μL of HRP-conjugated GAM (1:2000) (Jackson ImmunoResearch Europe Ltd.) or HRP-conjugated sheep anti-human serum albumin (HSA-HRP) (Abcam) (1:2000) in PBS with 1% BSA or PBS with 1% NFDM were added to each well. The plates were washed and developed using 3,3′,5,5′-Tetramethylbenzidine (TMB, Sigma-Aldrich), reaction was stopped with 4N H_2SO_4 (Thermofisher Scientific) and the absorbance was measured at 450–570 nm using a Thermo Scientific Multiskan FC plate reader. Data was analyzed using GraphPad Prism 8.4.0 software.

Flow cytometry

$HEK293^{h4-1BB}$ or $HEK293^{m4-1BB}$ cells, and $3T3^{hEGFR}$ cells (2.5×10^5 cells/well) were incubated on ice for 30 min with purified antibodies (5 μg/mL), washed and incubated with anti-FLAG mAb (5 μg/mL) (clone M2; F3165, Sigma-Aldrich) for 30 min and detected with a phycoerythrin (PE)-GAM IgG F(ab') antibody (Jackson ImmunoReserach) (1:200 dilution). HEK293 and 3T3 cells were used as controls. Samples were analyzed with FACSCanto II cytometer (BD Biosciences) and FlowJo X software was used for analyzing flow cytometry data.

FcRn binding kinetics assessment by Bio-Layer Interferometry

An Octet Red96e system (Sartorius) was used for Bio-Layer Interferometry (BLI) to investigate FcRn binding kinetics. Streptavidin coated biosensors (Sartorius) were hydrated in PBS with 0.01% (v/v) Tween 20 (Bio-Rad) at pH 7.4 followed by immobilization of 8.75 nM biotinylated human FcRn (Immunitrack) in PBS with 0.01% (v/v) Tween 20 and then washed in fresh PBS with 0.01% (v/v) Tween 20. For all analytes [FcRn high-binding albumin ($Albumin^{HB}$) (Bern et al., 2020), LiTCo-Albu and LiTCo] a 2-fold dilution series starting from 200 nM was prepared in kinetics buffer (PBS with 25 mM CH_3COONa, 25 mM NaH_2PO_4, 150 mM NaCl, and 0.01% (v/v) Tween 20 at pH 5.5). For each analyte a control with no analyte but FcRn-coated biosensors and a control with 200 nM analyte but uncoated biosensors were also included. Binding kinetics were analyzed at 30°C. After a 180 s baseline in kinetics buffer, analyte association was performed in sample wells for 300 s before dissociation for 600 s in kinetics buffer, followed by biosensor regeneration in PBS with 0.01% (v/v) Tween 20 for 240 s. The control well without analyte was used for baseline subtraction. In the Octet System Data Analysis software (version 10.0.1.6) a 1:1 binding model was used to determine kinetic parameters.

FcRn-mediated cellular recycling assay

The FcRn-mediated cellular recycling assay was performed according to Schmidt, Hvam et al. (Schmidt et al., 2017). HMEC-1-FcRn cells were trypsinized, suspended in medium, centrifuged at 300 G for 5 min, and resuspended. Cells (1×10^5/well) were seeded in a 48-well plate (Sarstedt) previously coated with GelTrex (Life Technologies) and incubated until near confluent. 150.4 nM analyte samples (LiTCo-Albu and FcRn wild-type-binding albumin, and AlbuminHB (Bern et al., 2020) were prepared in Hank's Balanced Salt Solution (Sigma-Aldrich) adjusted to pH 6.0 with MES buffer (Sigma-Aldrich). HMEC-1-FcRn cells were washed twice with warm PBS before incubation with 300 μL analyte for 1 h at 37°C, 5% CO_2. Cells were then washed 5 times with ice-cold PBS, before incubation with 160 μL serum-free medium for 1 h. The supernatant was harvested, and the amount of recycled analyte was quantified by sandwich ELISA. 96-well plates (NUNC Brand Products) were coated with capture antibody (Sigma-Aldrich) 1:1000 in PBS for 2 h at room

temperature and then blocked with 2% NFDM in PBS for 2 h at room temperature. The wells were washed in PBS with 0.05% (v/v) Tween 20 before incubation overnight at 4°C with recycling samples and corresponding dilution series of albumin and LiTCo-Albu. Wells were washed again and then incubated for 2 h at room temperature with anti-HSA-HRP detection antibody diluted 1:5000 in PBS with 2% NFDM. The wells were then washed and TMB (Kem-En-Tec) added. The reaction was stopped with 0.2 M H_2SO_4 and the absorbance at 450 nm was measured with a Clariostar plate reader (BMG Labtech) with background subtraction of the absorbance at 655 nm. The data was analyzed using GraphPad Prism 9.0.0 software.

4-1BB-dependent NF-kB activation assay

4-1BB-dependent activation of activated nuclear factor kappa-B (NF-κB) assay was performed on thaw-and-use (T&U) GloResponseTMNFkB-luc2/4-1BB Jurkat cells (Promega) according to the manufacturer's instructions. Jurkat cells (1.5 × 105 cells/well) were plated in Assay Buffer (RPMI, Gibco with 1% FBS) in white flat bottom 96-well plate (Sigma-Aldrich) co-cultured with NIH/3T3 cells that express or not hEGFR (0.3 × 105 cells/well). The hLiTCo, hLiTCo-Albu or control antibody were added at 10-fold serial dilutions. After 6 h Bio-Glo Luciferase Assay Reagent (Promega) was added and luciferase activity was assessed using a Tecan Infinite F200 plate-reading luminometer (Tecan Trading). The experiments were performed in triplicates and data are reported as x-fold of induction relative to the values obtained from unstimulated cells (mean ± SD). Data was analyzed and plotted using GraphPad Prism 8.4.0 software.

Antigen specific T cell costimulation assay

3T3 and $3T3^{hEGFR}$ cells (0.3 × 105 cells/well were pre-coated in 96-well plates overnight at 37°C. Next day, target cells were pre-incubated for 1 h at 37°C with purified antibodies (6.67 nM) and a mouse IgG1K isotype (Biolegend), as a control. Mouse CD8a+ T cells were purified from the spleens of female BALB/c mice using the mouse CD8a+ T cell Isolation Kit (Miltenyi Biotec). Purified mouse CD8a+ T cells (1 × 105 cells/well) were resuspended in RPMI supplemented with 10% FBS and 50 μM β-mercaptoethanol (Life Technologies), activated with anti-CD3 mAb (clone 145-2C11; MO3PU, Immuno-step) (1 μg/mL) and added to the coculture. As a control, mouse CD8a+T cells were cultured alone with or without anti-CD3 mAb (1 μg/mL). After 72 h supernatants were collected and assayed for IFN-γ secretion by ELISA (Diaclone) following manufacturer's protocol.

Serum stability

Purified mLiTCo and mLiTCo-Albu were incubated in mouse serum (Invitrogen) at 37°C, for at least 7 days. The binding activity of the sample at 0 h was set as 100% in order to calculate the time corresponding to percentage of decay in binding activity. Samples were analyzed with Thermo Scientific Multiskan FC photometer and GraphPad Prism 8.4.0 software.

Pharmacokinetics study

Female BALB/c mice were intravenously (i.v.) injected (tail vein) with a single dose (2 mg/kg) of mLiTCo (n = 3), mLiTCo-Albu (n = 4) or PBS (n = 3). Blood samples were collected at 5 min, 3, 24, 48, 98 and 168 h in separation gel BD microtubes (BD Biosciences), centrifuged at 5000 rpm for 1.5 min to obtain serum and stored at −20°C. To determine antibody concentration, sera were analyzed by ELISA against m4-1BB Fc chimera (m4-1BB, SinoBiological) plastic immobilized (3 μg/mL). After washing and blocking in PBS with 5% NFDM, sera from different time points were added and incubated 1 h at room temperature. After washing, HRP-conjugated anti-FLAG mAb (clone M2; ab49763, Abcam) (1 μg/mL) was added, after which the plates were washed and developed using TMB, reaction was stopped with 4N H_2SO_4 and the absorbance was measured at 450–570 nm using a Thermo Scientific Multiskan FC plate reader. Data was analyzed using GraphPad Prism 8.4.0 software.

Therapeutic studies

$CT26^{hEGFR}$ cells (1.5 × 10^6/mouse) were implanted subcutaneously (s.c.) into the dorsal space of 6-week-old female BALB/c mice. Mice were treated every other day for a total of seven intraperitoneal (i.p.) injections of PBS or mLiTCo-Albu (3 mg/kg) antibodies and a weekly i.p. dose of anti-4-1BB IgG (clone 3H3; BE0239, BioXCell) (4 mg/kg) for two weeks. On days 0 and 21 mice were anesthetized and bled to obtain mouse serum in separation gel BD microtubes, after centrifugation serum was stored at −20°C until use. Levels of inflammatory cytokines (IFN-γ and IL-6) from collected serum were analyzed by ELISA (Diaclone and Abcam, respectively) following manufacturer's protocol. In the combined immunotherapy *in vivo* assay

$CT26^{hEGFR}$ cells (1.5×10^6/mouse) were implanted s.c. into the dorsal space of 6-week-old female BALB/c mice. Mice were treated every other day for a total of six i.p. injections of PBS or mLiTCo-Albu alone, or in combination with two weekly i.p. injections of anti-PD-1 IgG (clone RMP 1.14; BE0146, BioXCell) (4 mg/kg). In both studies tumor growth was monitored by caliper measurements three times a week, and when tumors reached approximately 0.3–0.4 cm in diameter (0.014–0.03 cm^3 in volume), mice were randomized and allocated to receive treatment (n = 5–6/group). Measurements were conducted in a random order by the investigator who was blinded to the treatment assignment. Mice were euthanized when tumor size reached a diameter of 1.5 cm any dimension, when tumors ulcerated, or at any sign of mouse distress.

QUANTIFICATION AND STATISTICAL ANALYSIS

Statistical analysis

Statistical analysis was performed using the GraphPad Prism Software version 8.4.0. and 9.0.0. All the *in vitro* experiments were done in triplicates and values are presented as mean ± SD from one of at least three separate experiments. Significant differences (p value) were discriminated by applying a two-tailed, unpaired Student's *t* test assuming a normal distribution. p values are indicated in the corresponding figures. Tumor volumes for individual mice in each treatment group are plotted, and the mean tumor volumes are presented for each group using a scatterplot as mean ± SD Differences in tumor growth were determined by one-way analysis of variance (ANOVA) adjusted by the Bonferroni correction for multiple comparison tests.